Wollongong to Ann Arbor

WolframAlpha computational knowledge engine

wollongong to ann arbor

Input interpretation:

Wollongong, New South Wales, Australia to Ann Arbor, Michigan

Distance: Show metric units

9477 miles

Map:

Fraction of Earth circumference:

0.38 ≈ 1 / 3

Direct travel times:

aircraft (550 mph)	17 hours 10 minutes
sound	12 hours 30 minutes
light in fiber	71.3 ms (milliseconds)
light in vacuum	50.9 ms (milliseconds)

(assuming constant–speed great–circle path)

Presentation scheduled start time:

Ann Arbor 11 am EDT, Thursday, July 15, 2010

Wollongong 1 am EST, Friday, July 16, 2010

The nature of terahertz emission from GaAsBi

Roger Lewis

Institute for Superconducting and Electronic Materials,
University of Wollongong, Australia

THz: seeing the unseen

Fluorescent marker pen: lid on

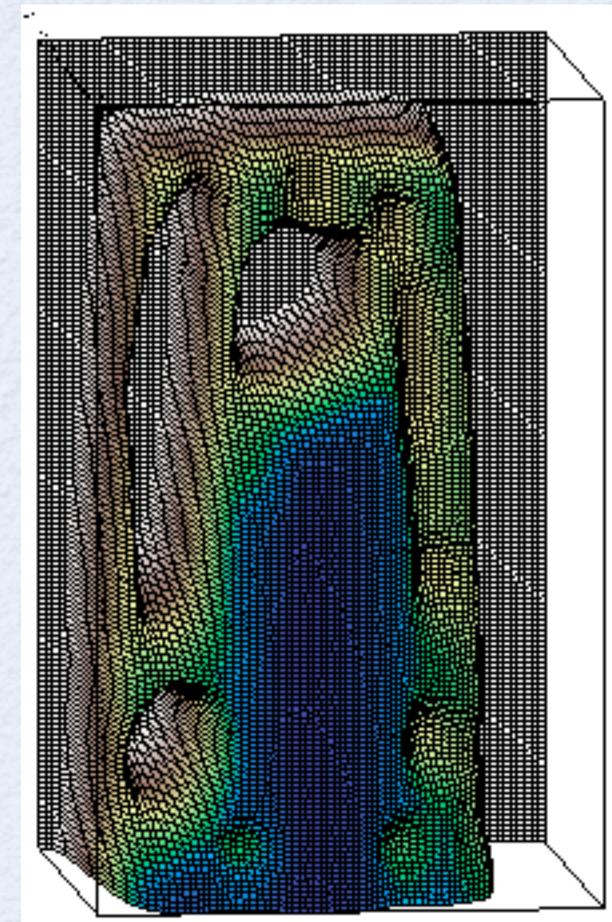

bolo

Cameron Lee
2009

THz: seeing the unseen

Bubble wrap: one bubble with water

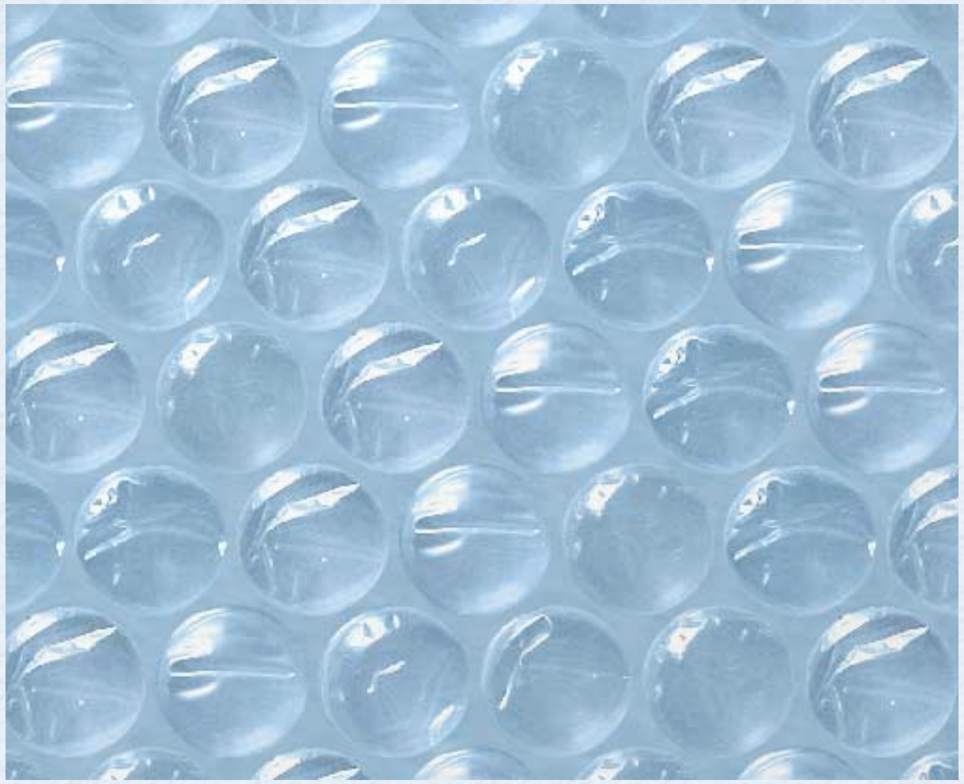

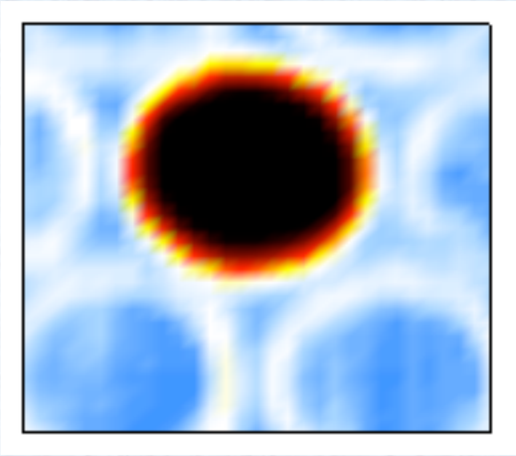

pyro

Cameron Lee
2009

THz: seeing the unseen

invisible

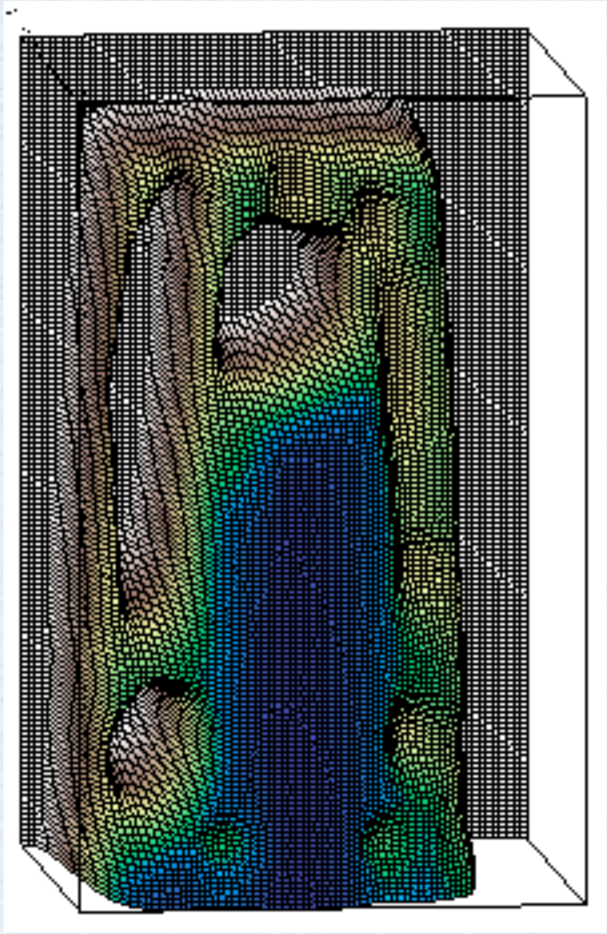

Eye does not see through lid

invisible

Eye sees through water

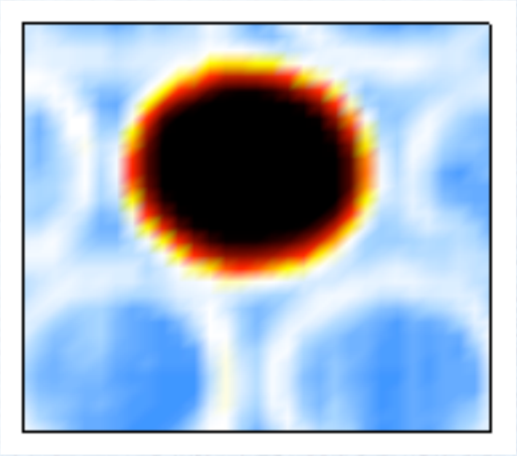

700 nm

428 THz

400 nm

749 THz

Chart of the Electromagnetic Spectrum

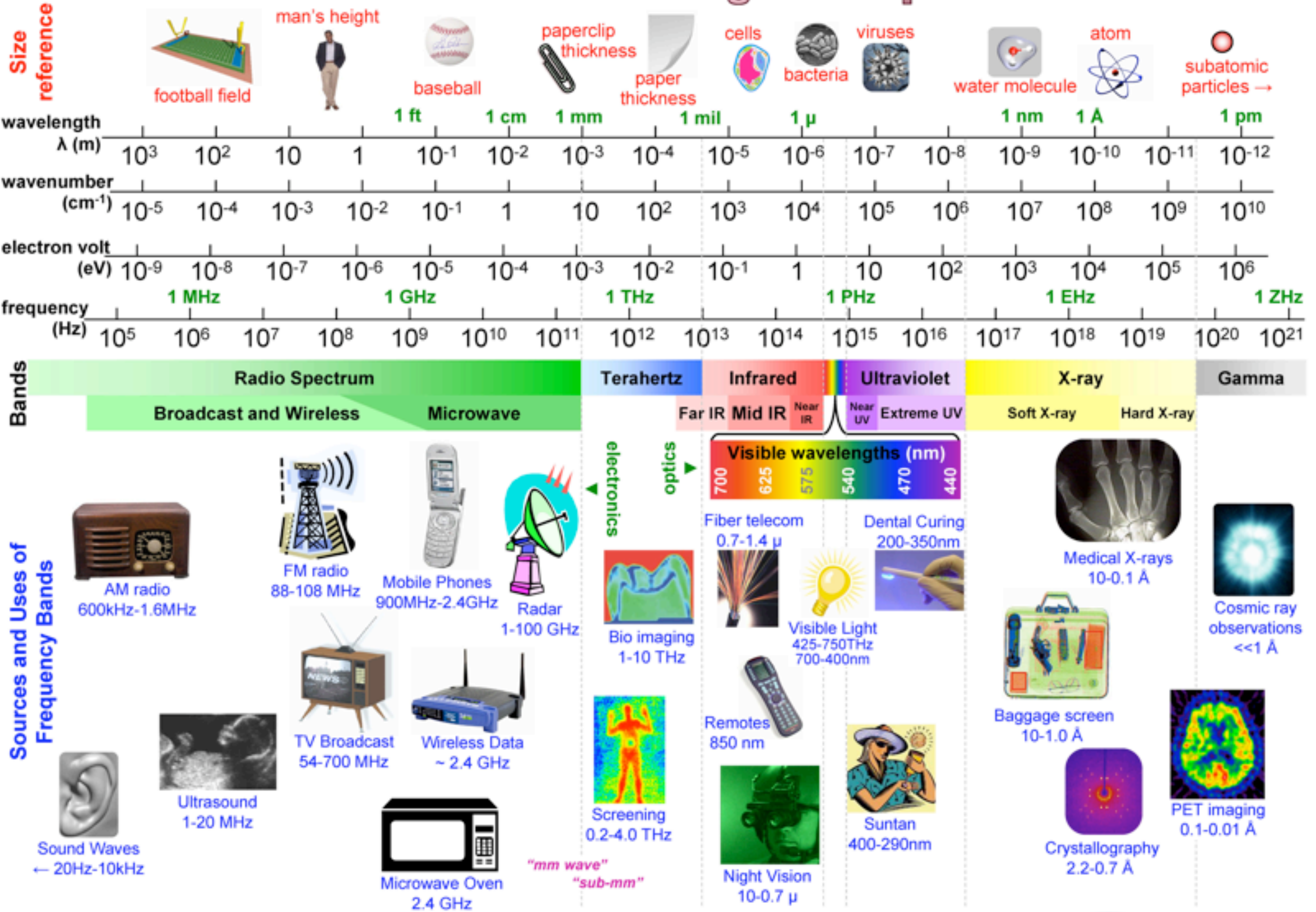

$\lambda = 3x10^8/freq = 1/(wn*100) = 1.24x10^{-6}/eV$

SURA Southeastern Universities Research Association ®

Overview of THz @ UOW; 1 of 4

Blackbody radiation

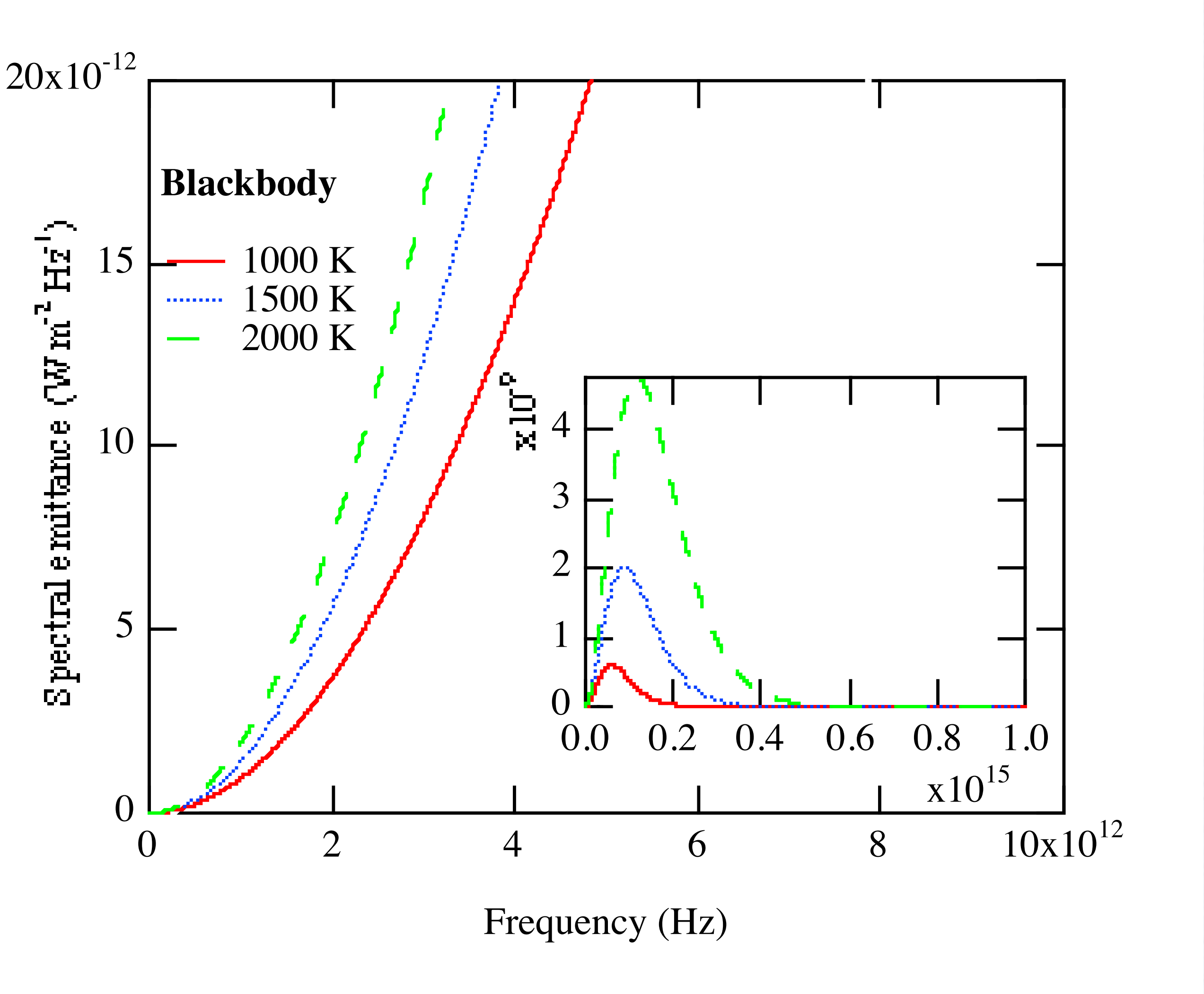

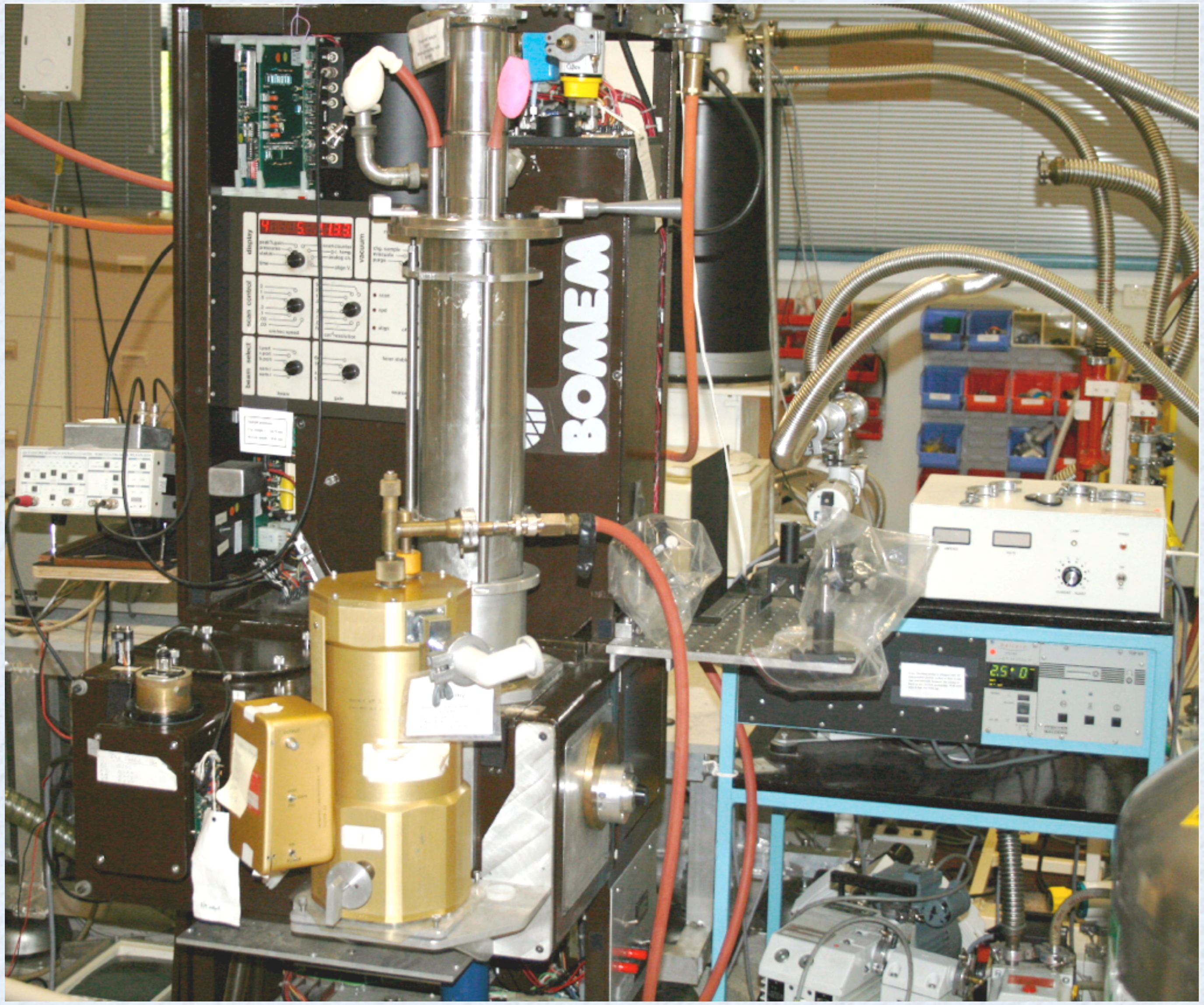

Overview of THz @ UOW; 2 of 4

Far-infrared (THz) laser

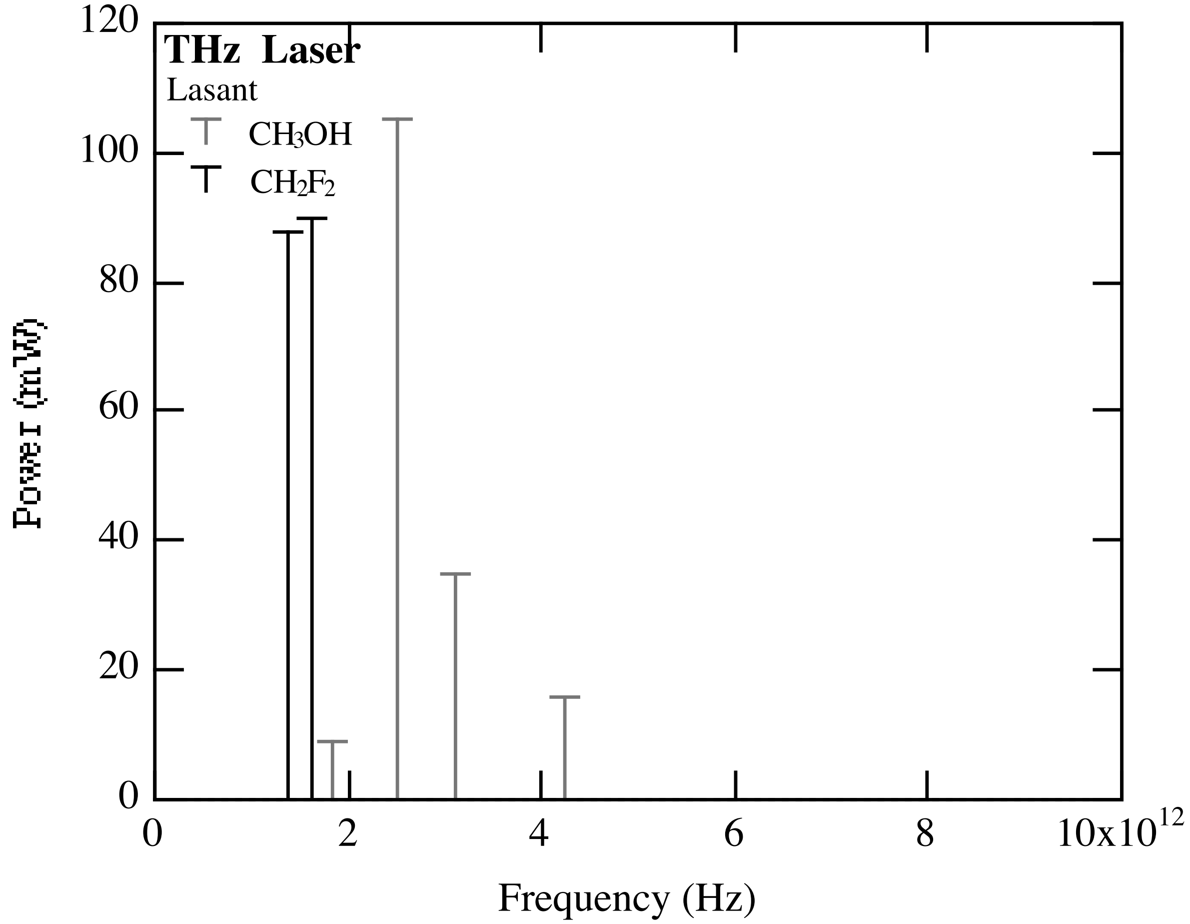

S. Hargreaves and R. A. Lewis
Journal of Materials Science: Materials in Electronics **18**, S299 (2007)

Overview of THz @ UOW; 3 of 4

Two-colour photomixing

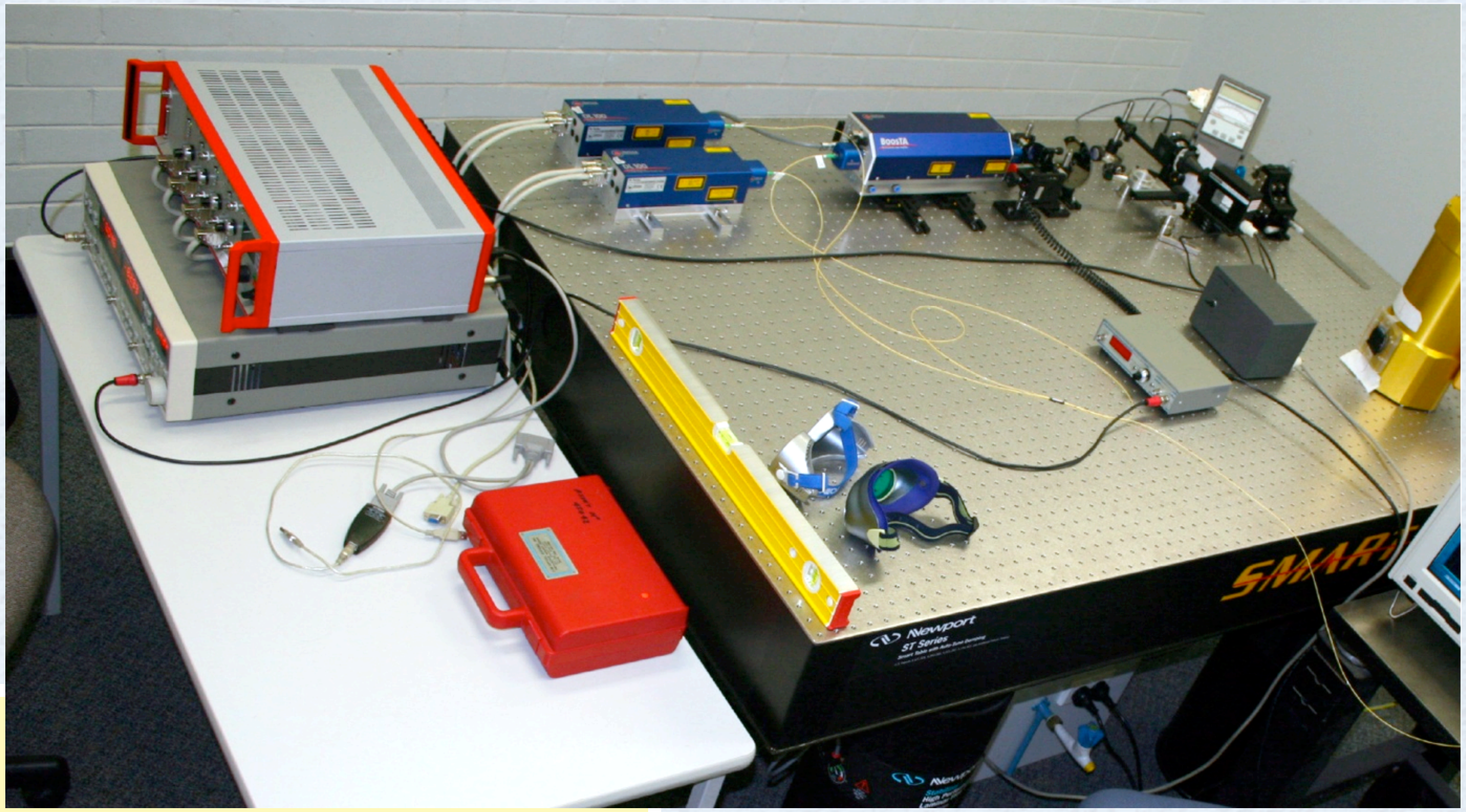

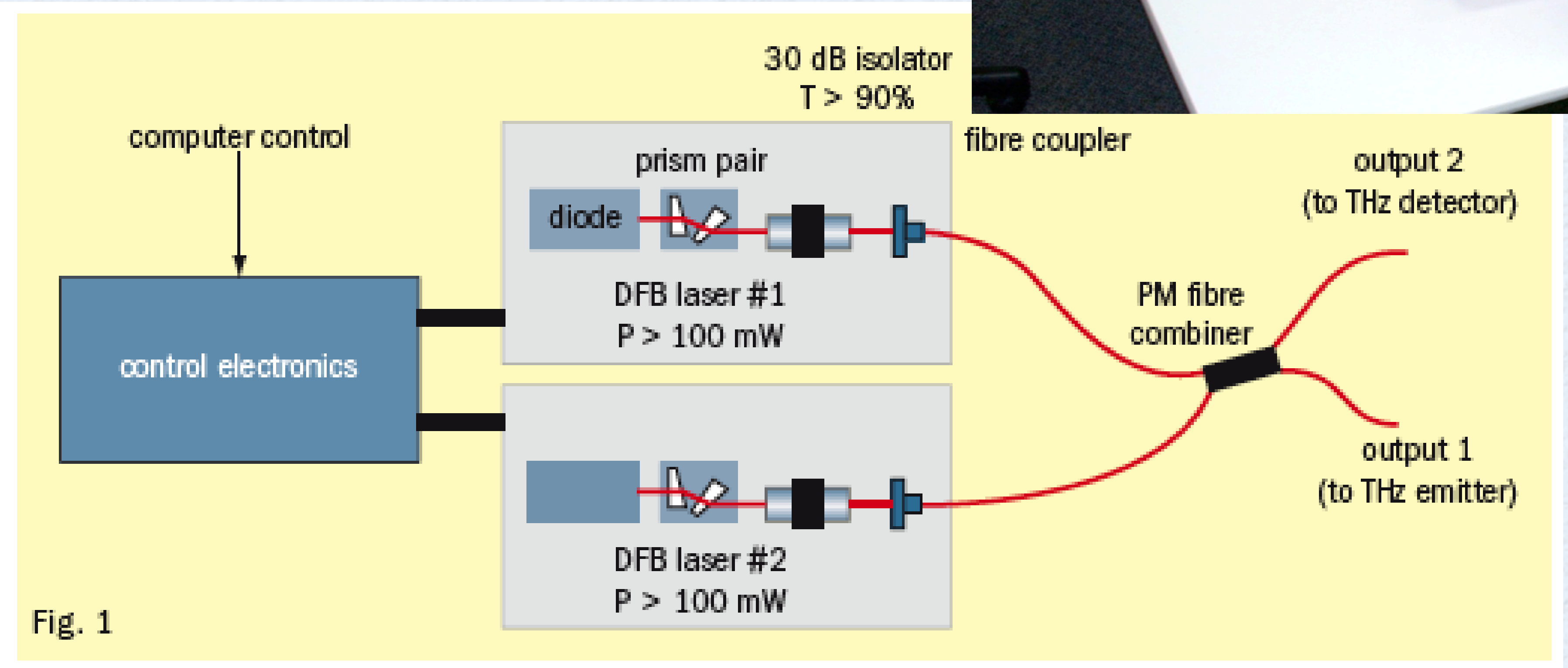

Fig. 1

Graphic: Toptica

Overview of THz @ UOW; 4 of 4

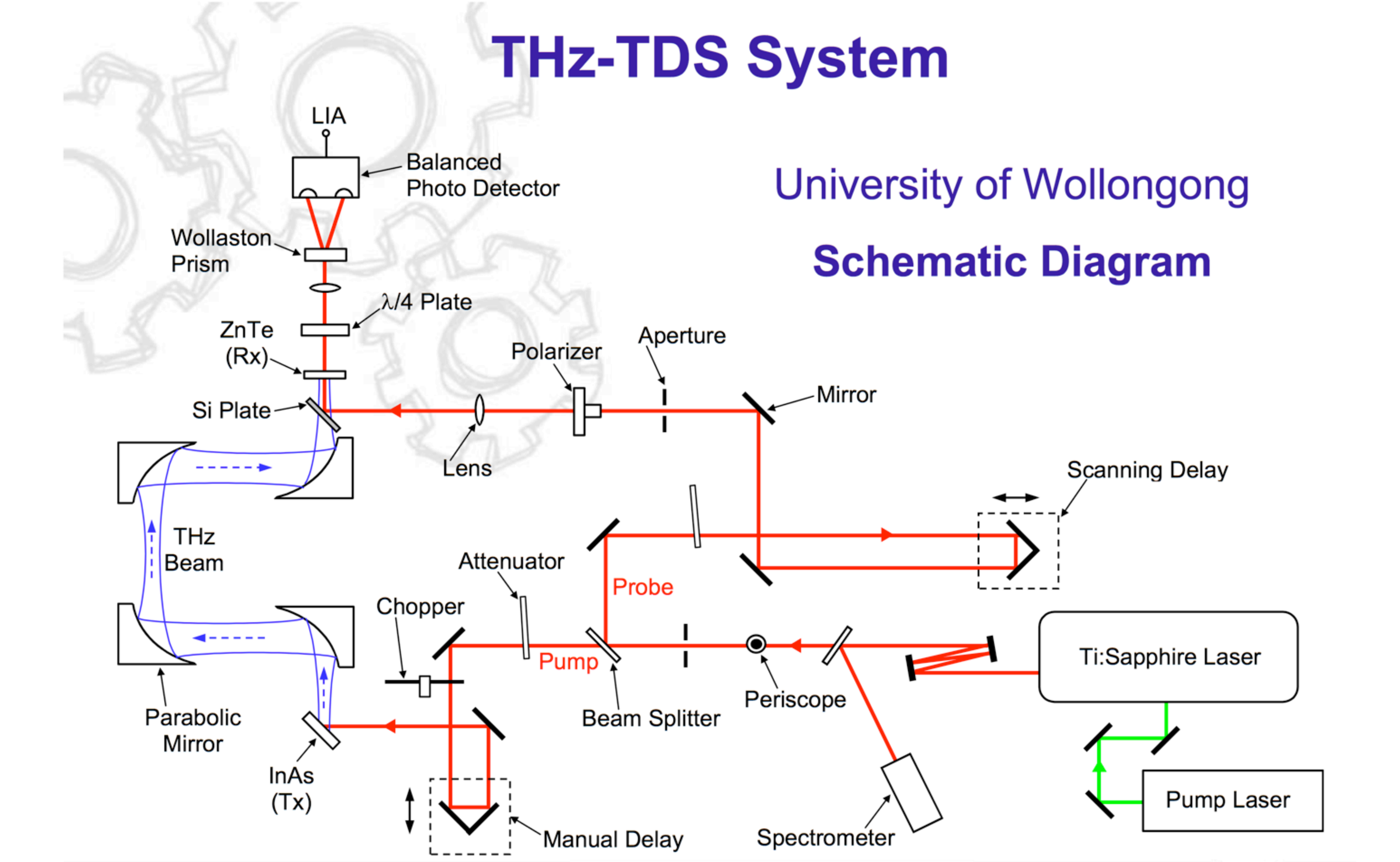

Graphic: R. Mendis

Ultrashort pulses induce polarization

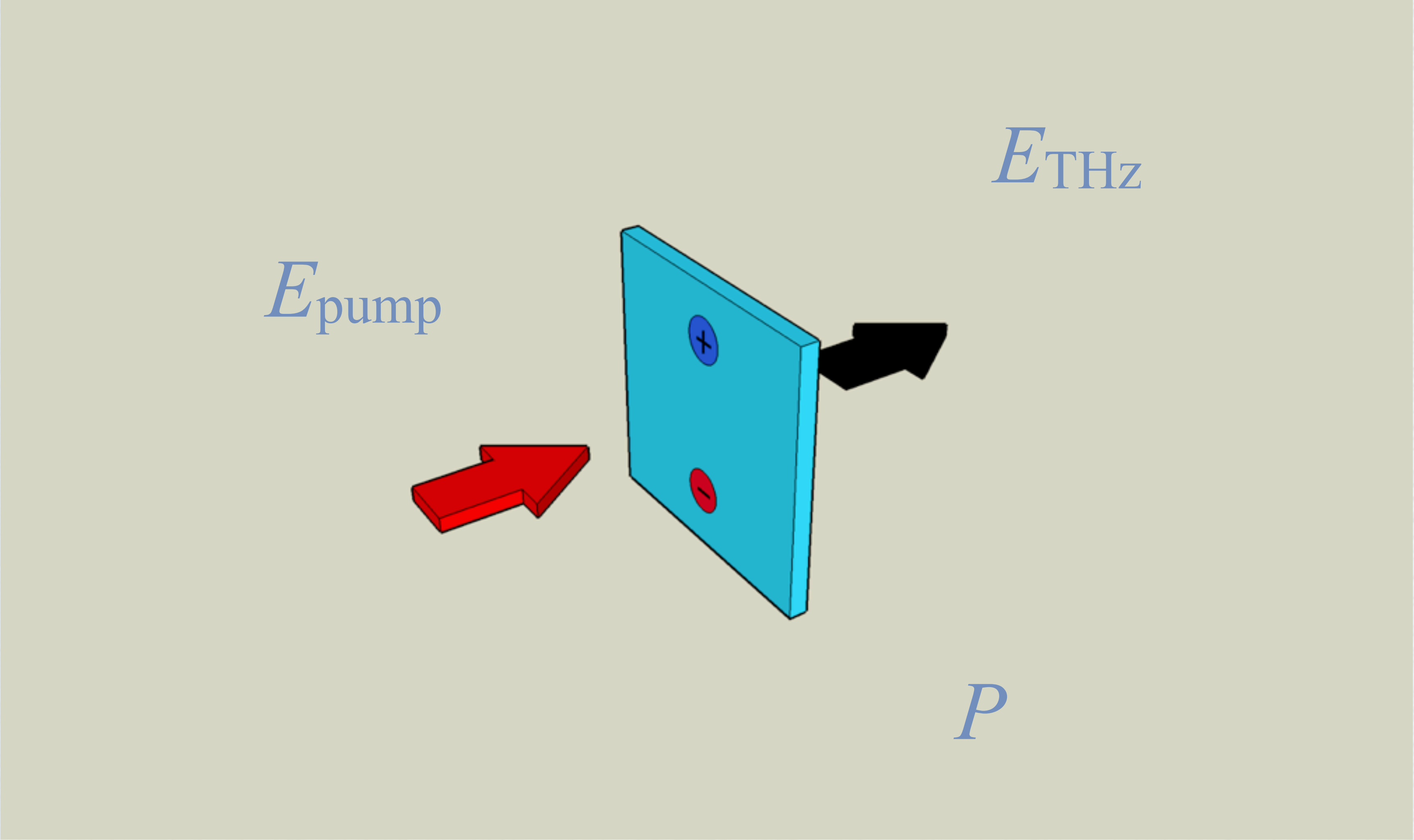

Graphic: A. Lewis

THz generation by ultrashort pulses

mechanisms

Photoconductivity (PC)

Transient Current (TC)

Optical Rectification (OR)

methods

geometry

polarization

pump-beam power

magnetic field

temperature

bias control

Evidence for Transient Currents

In-plane **magnetic field** rotates radiating dipole

Saturation with **excitation fluence** - carrier screening

FIG. 3. (Color online) Terahertz emission from nominally undoped InP as a function of magnetic field (main figure) and of excitation fluence (inset). The magnetic field is provided by a permanent magnet behind the sample. The magnetic field direction is in the sample plane. The magnetic field angle is measured counterclockwise around the pump beam starting from the incidence-reflection plane. Excitation fluence is ~0.2 $\mu J/cm^2$. Inset: terahertz emission in the absence of magnetic field as a function of excitation fluence.

S. Hargreaves, R. A. Lewis
Applied Physics Letters
93, 242101 (2008)

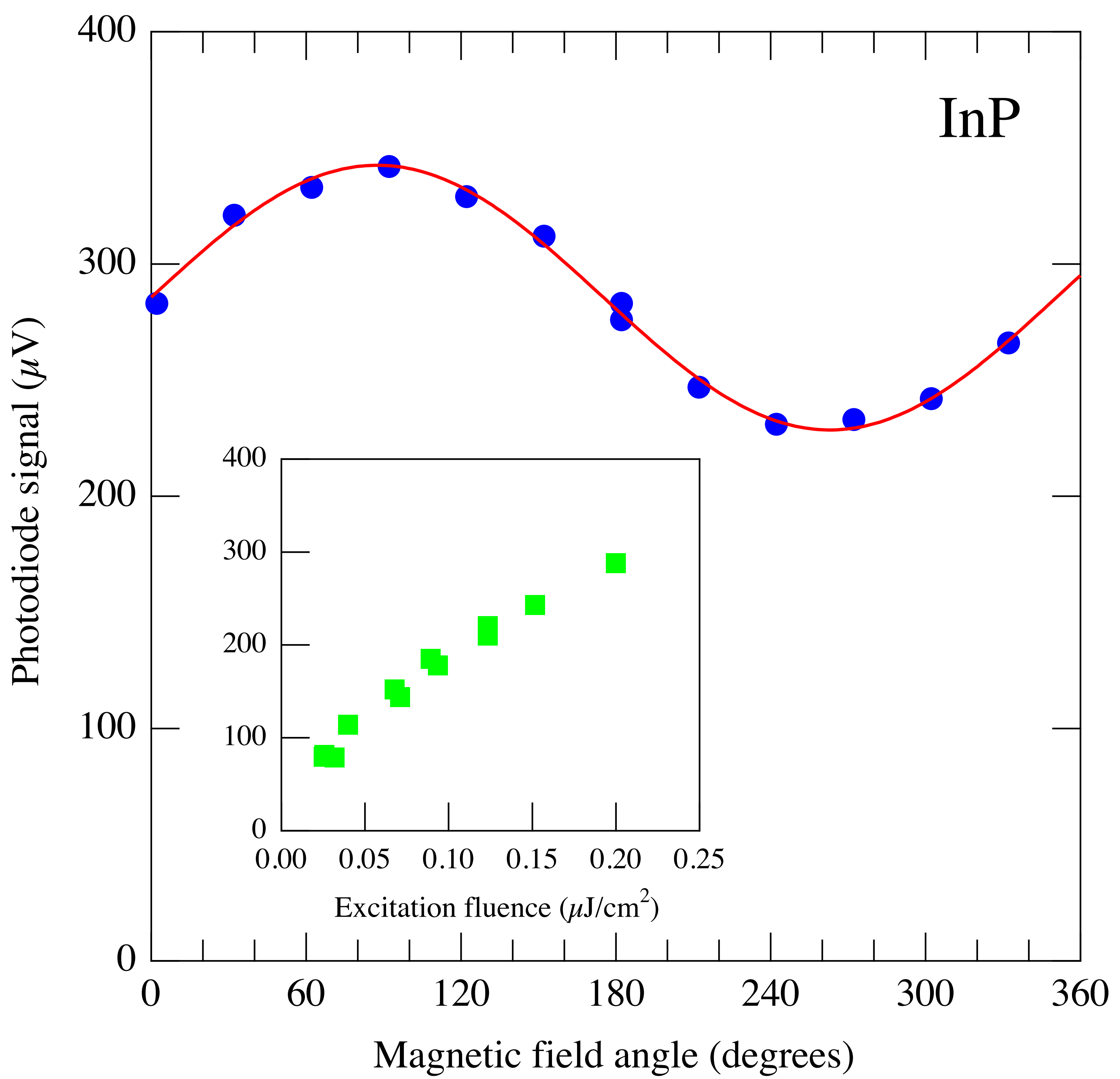

Optical Rectification - geometry

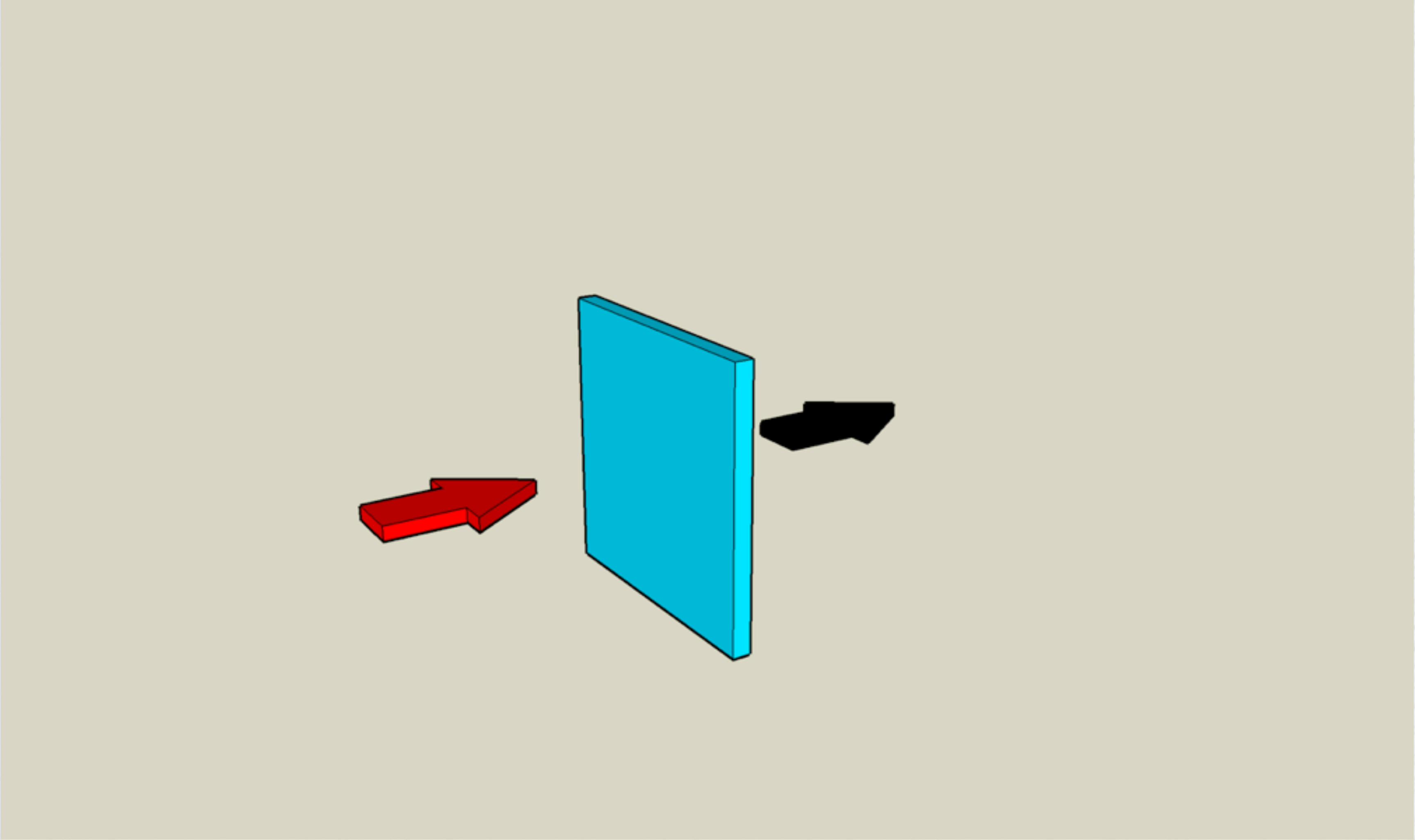

Graphic: A. Lewis

Optical Rectification - geometry

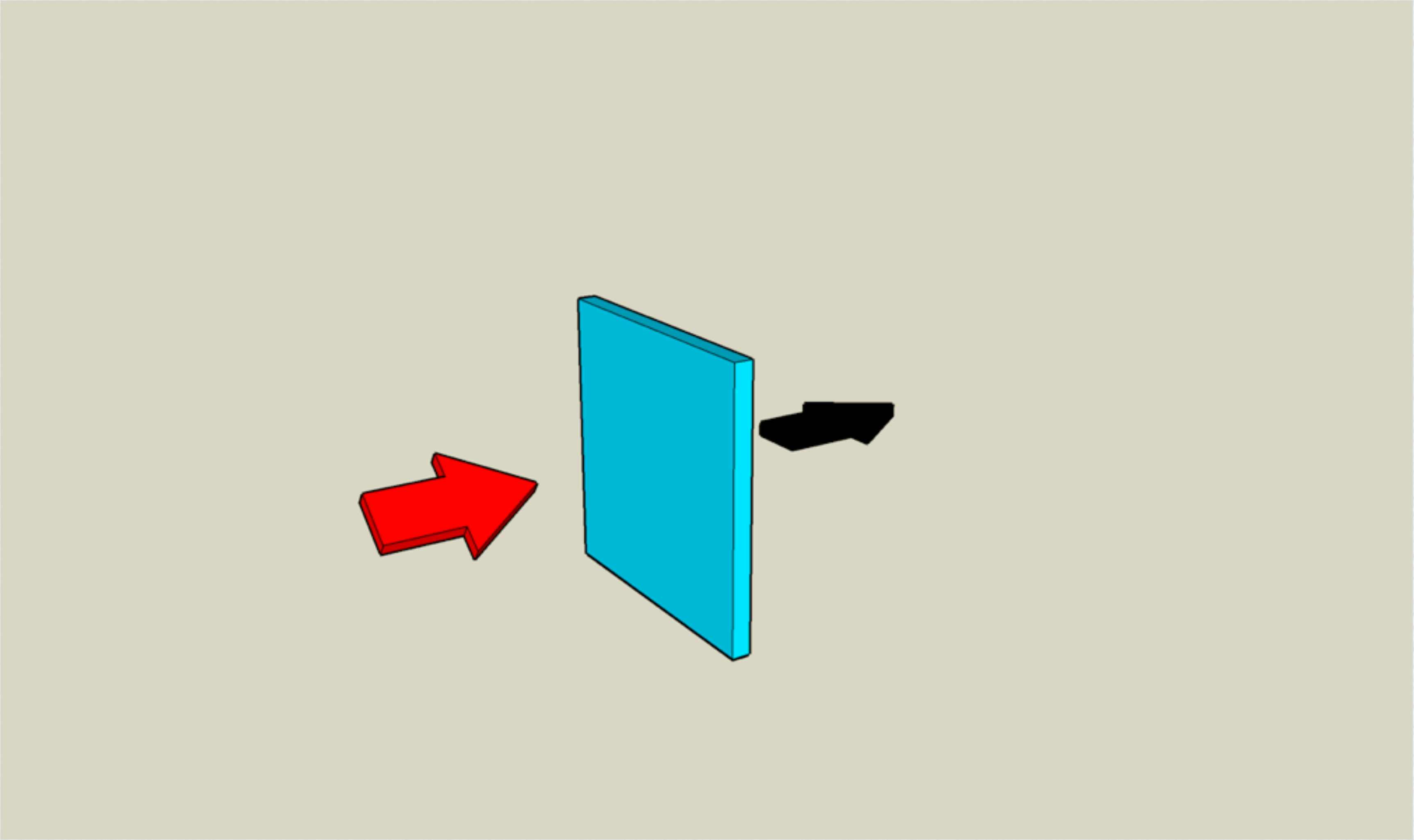

Graphic: A. Lewis

Optical Rectification - geometry

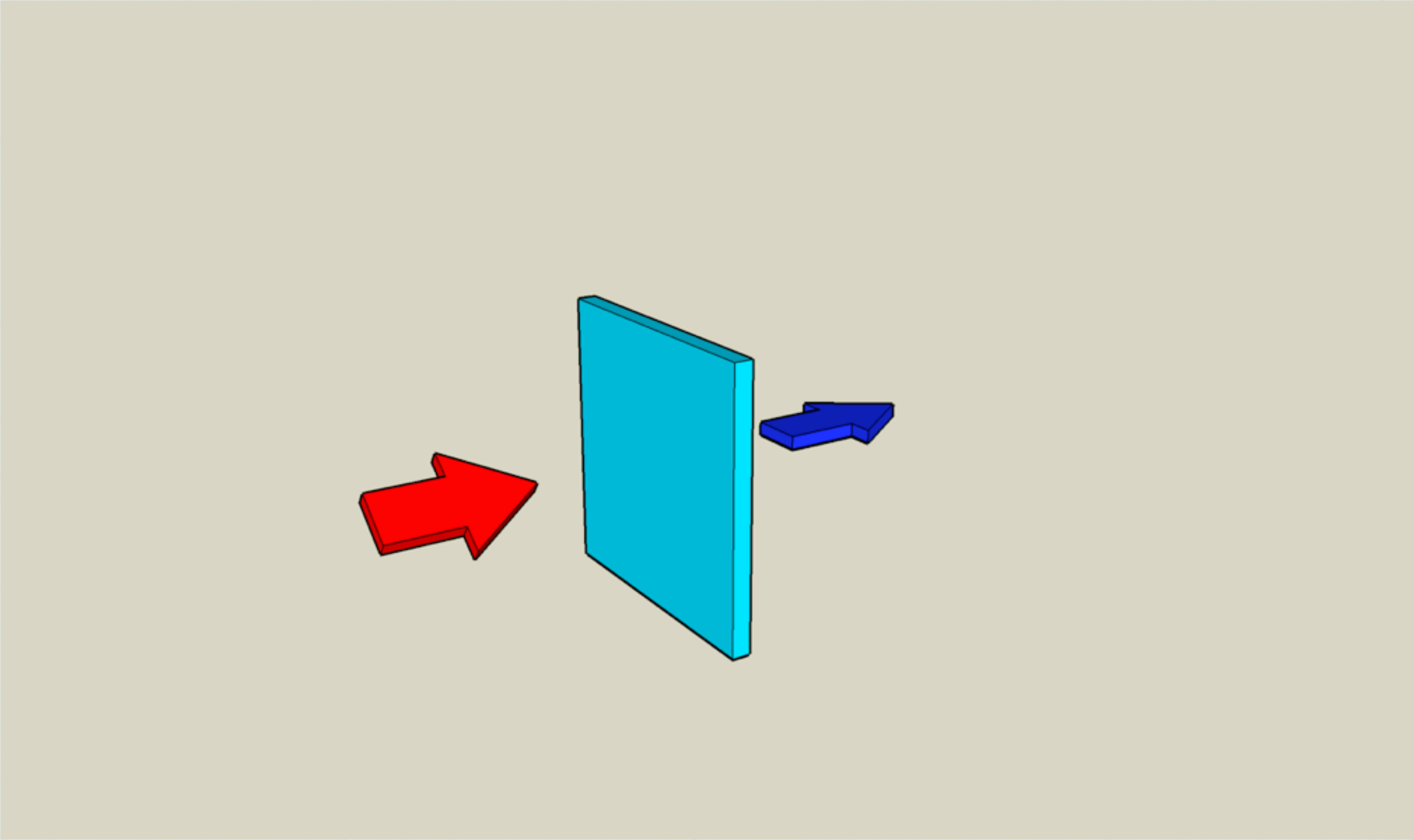

Graphic: A. Lewis

Optical Rectification - geometry

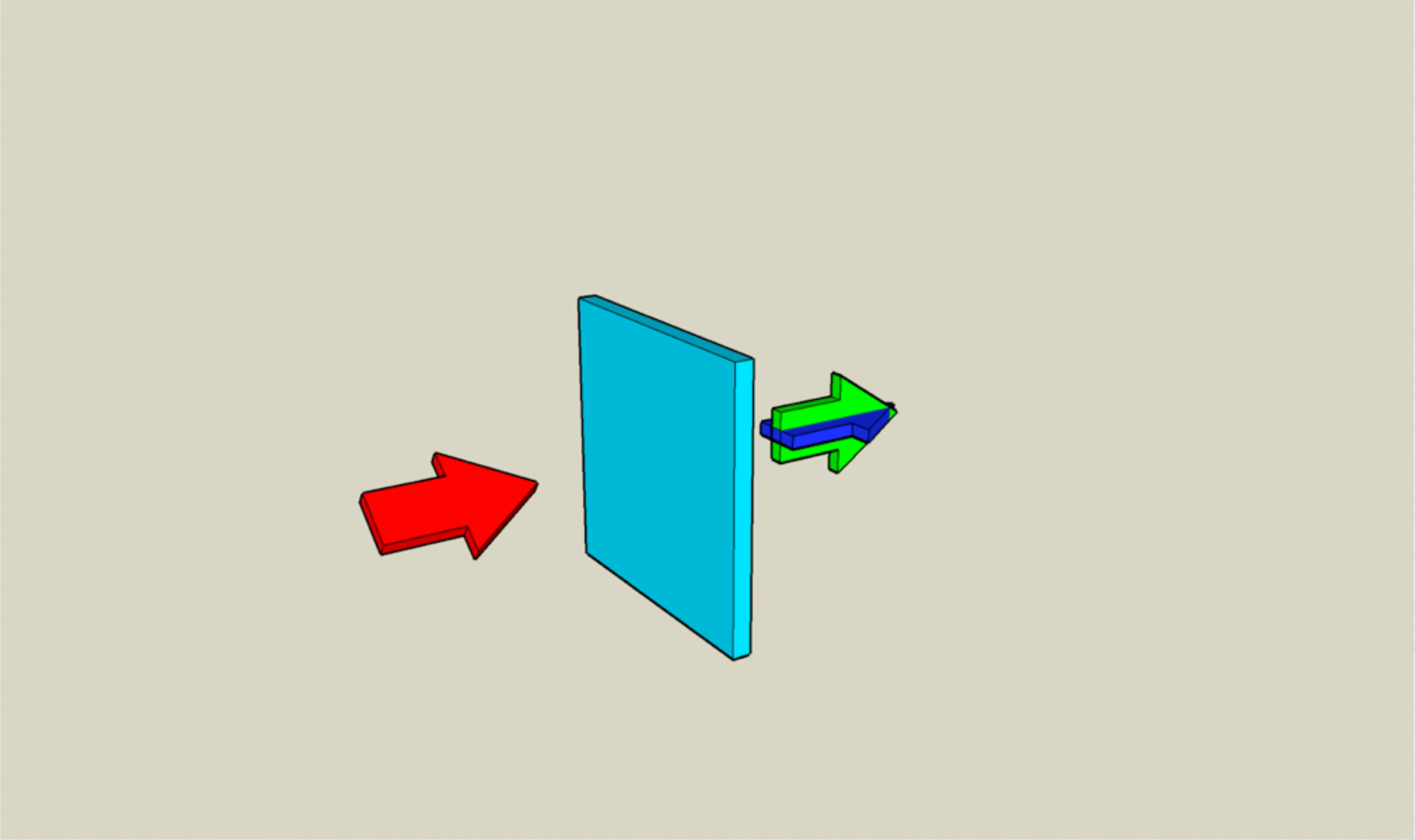

Graphic: A. Lewis

Optical Rectification - geometry

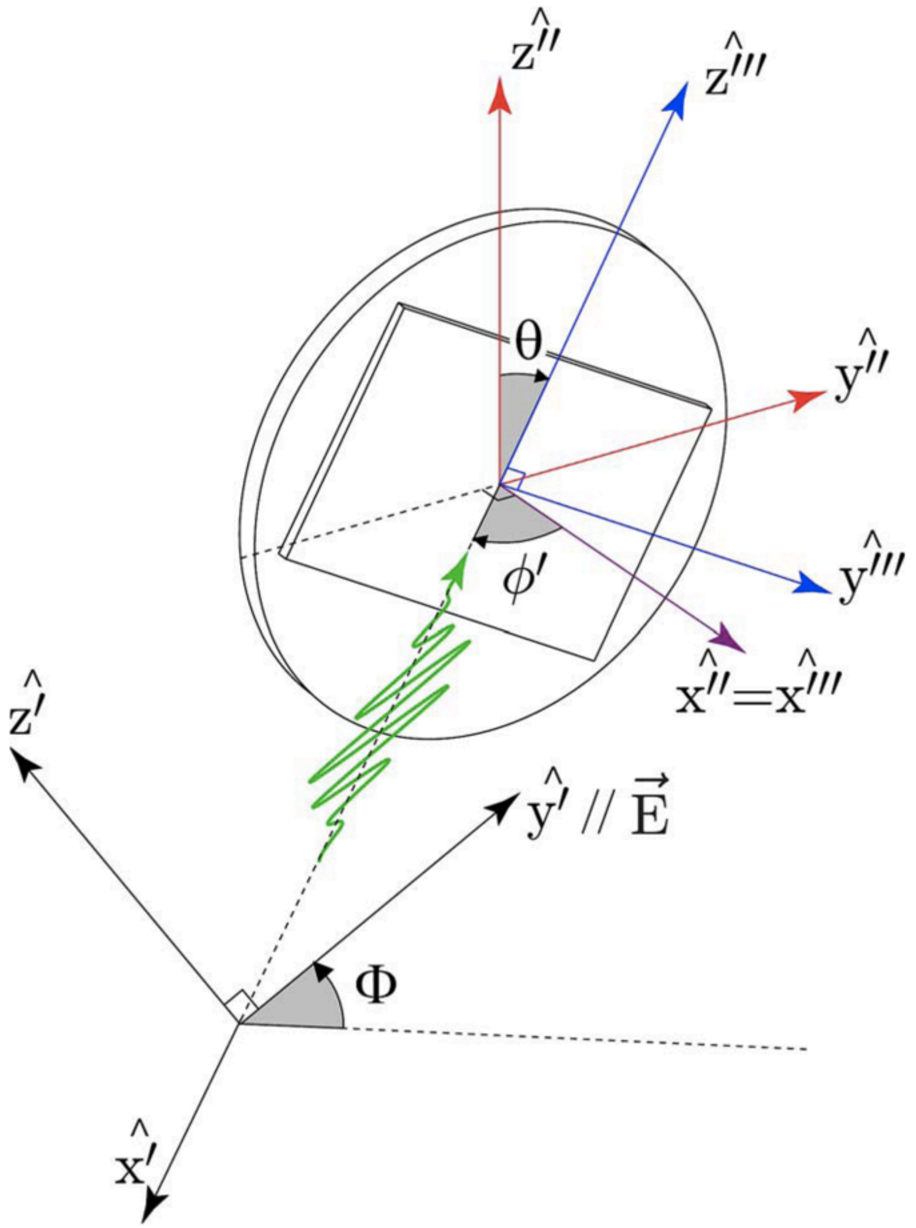

FIG. 1. (Color online) Coordinate axes and angles used. The incident radiation propagates in the $-\widehat{\mathbf{x}'}$ direction and is polarized in the $\widehat{\mathbf{y}'}$ direction. The outward-pointing normal to the crystal surface is given by $\widehat{\mathbf{x}''}$. The triple-primed axis system rotates with the crystal. The angle of incidence is ϕ'. The angle of polarization is Φ. The azimuthal angle is θ.

HARGREAVES, RADHANPURA, AND LEWIS

PHYSICAL REVIEW B **80**, 195323 (2009)

Optical Rectification - geometry

$$\begin{bmatrix} P_x''^{(bulk)} \\ P_y''^{(bulk)} \\ P_z''^{(bulk)} \end{bmatrix} = 2\, d_{14}\, E_0^2 \begin{bmatrix} G_{11} & G_{12} & G_{13} & G_{14} & G_{15} & G_{16} & G_{17} \\ G_{21} & G_{22} & G_{23} & G_{24} & G_{25} & G_{26} & G_{27} \\ G_{31} & G_{32} & G_{33} & G_{34} & G_{35} & G_{36} & G_{37} \end{bmatrix} \begin{bmatrix} 1 \\ \cos\theta \\ \sin\theta \\ \cos 2\theta \\ \sin 2\theta \\ \cos 3\theta \\ \sin 3\theta \end{bmatrix}$$

GaAs - Optical Rectification

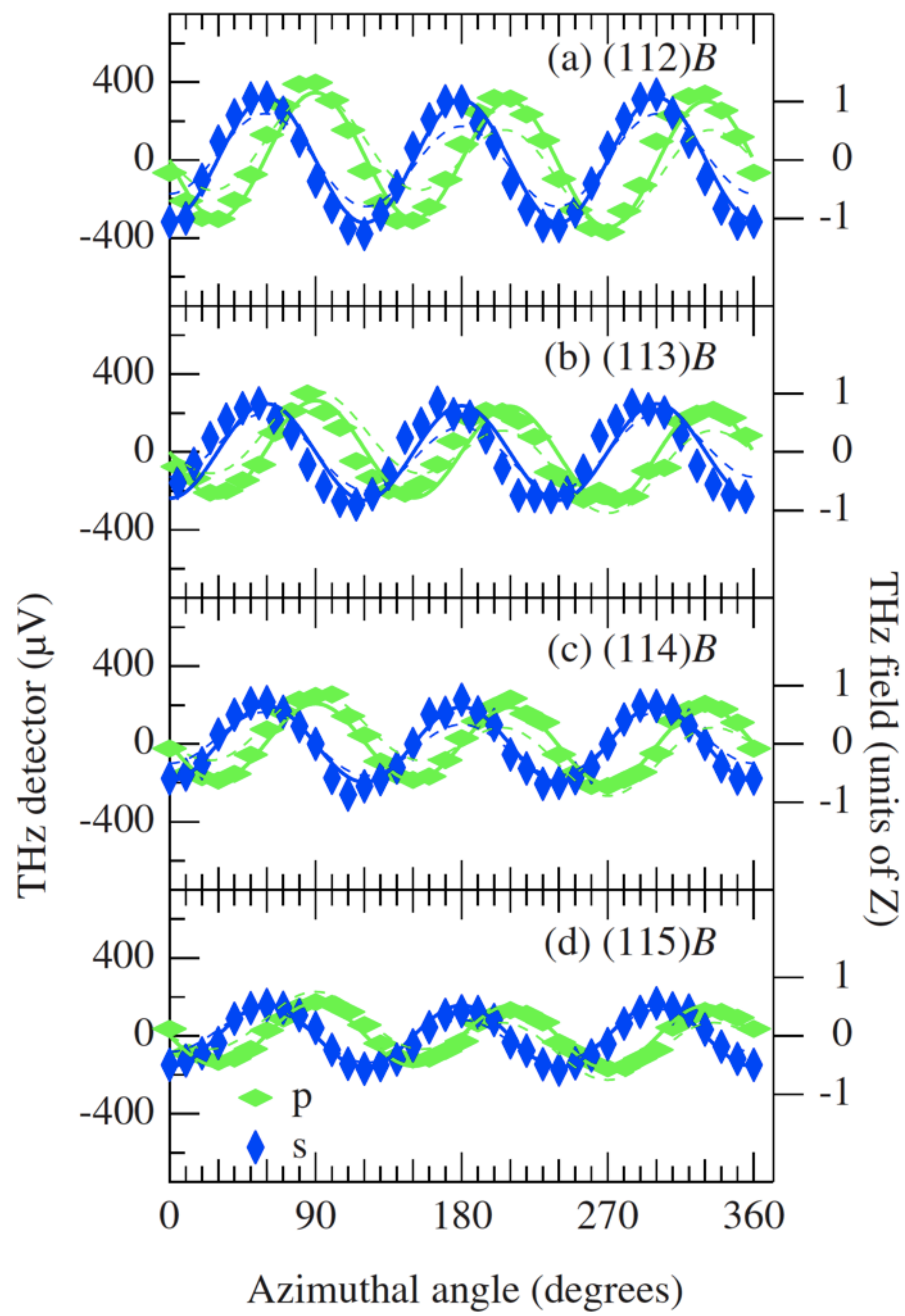

FIG. 3. (Color online) Experimental data (symbols) for THz emission from $(11N)B$ faces of GaAs. The dashed lines are the calculations for bulk optical rectification alone (with $d_{14}E_0^2=1$). The full lines are the calculations for combined bulk ($d_{14}E_0^2=1$) and surface ($\gamma' F_0=1.9d_{14}$) optical rectification.

GaAs - Optical Rectification

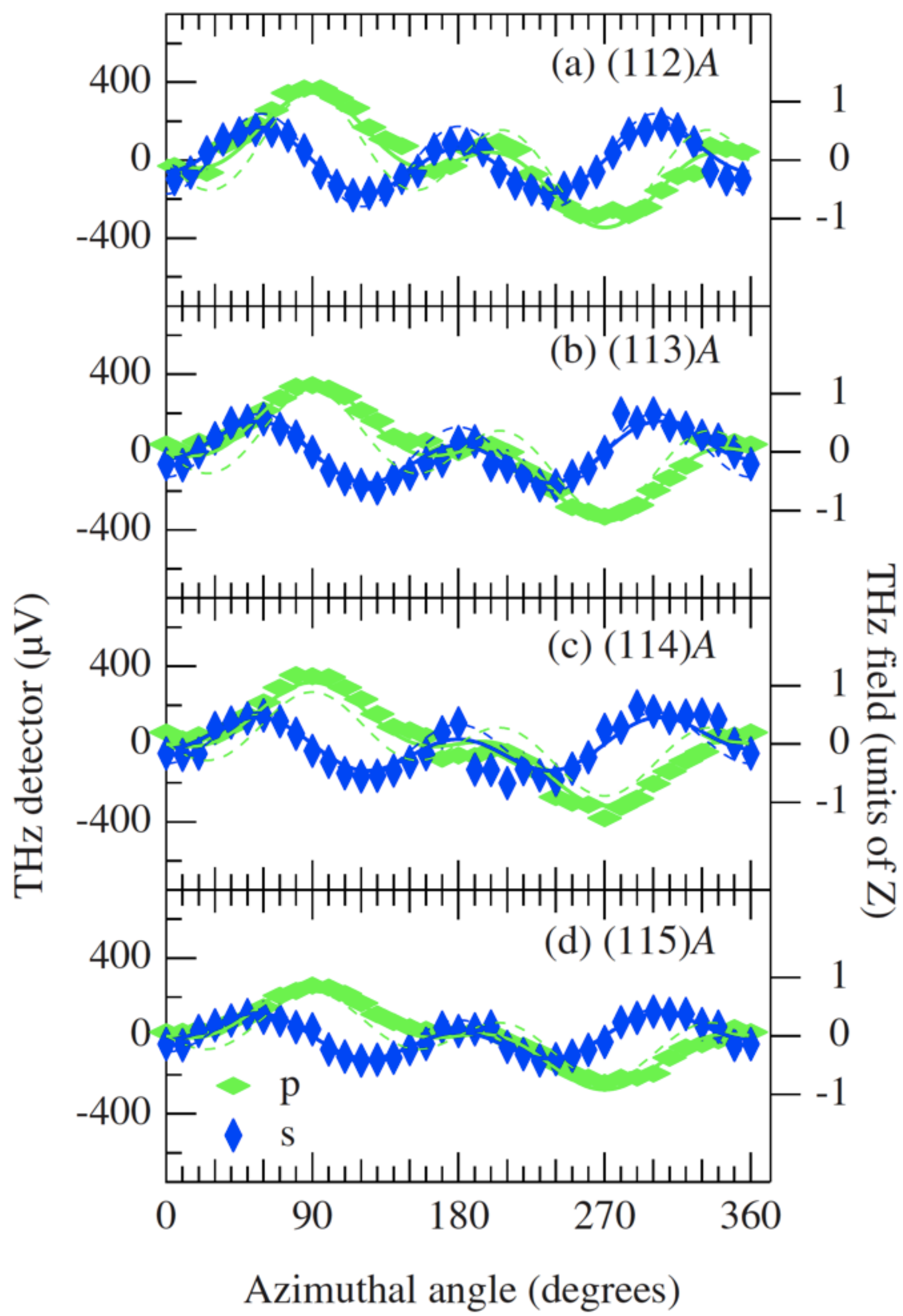

FIG. 4. (Color online) Experimental data (symbols) for THz emission from (11*N*)*A* faces of GaAs. The dashed lines are the calculations for bulk optical rectification alone (with $d_{14}E_0^2=1$). The full lines are the calculations for combined bulk ($d_{14}E_0^2=1$) and surface ($\gamma' F_0=-1.6d_{14}$) optical rectification.

GaBiAs

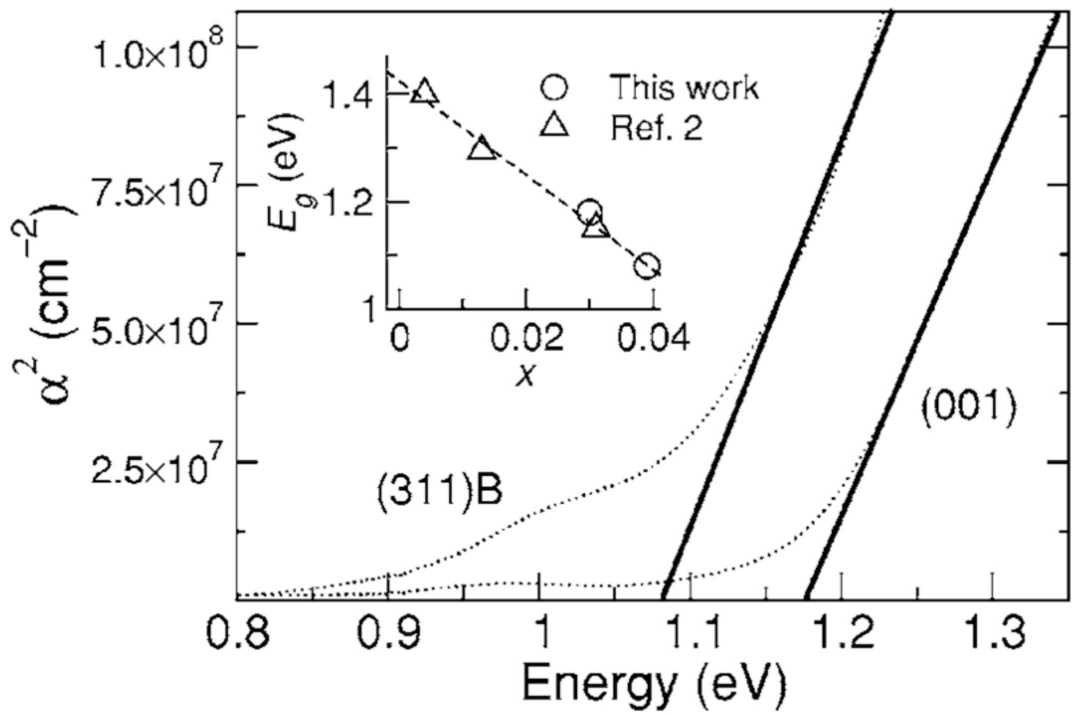

FIG. 3. Square of the absorption coefficient α^2 for the two near-stoichiometric (001) and (311)*B* $GaBi_xAs_{1-x}$ epilayers, obtained from transmission measurements at 300 K. Inset: Band-gap energy (E_g) vs x for these two samples, together with data from Ref. 2.

$GaBi_xAs_{1-x}$

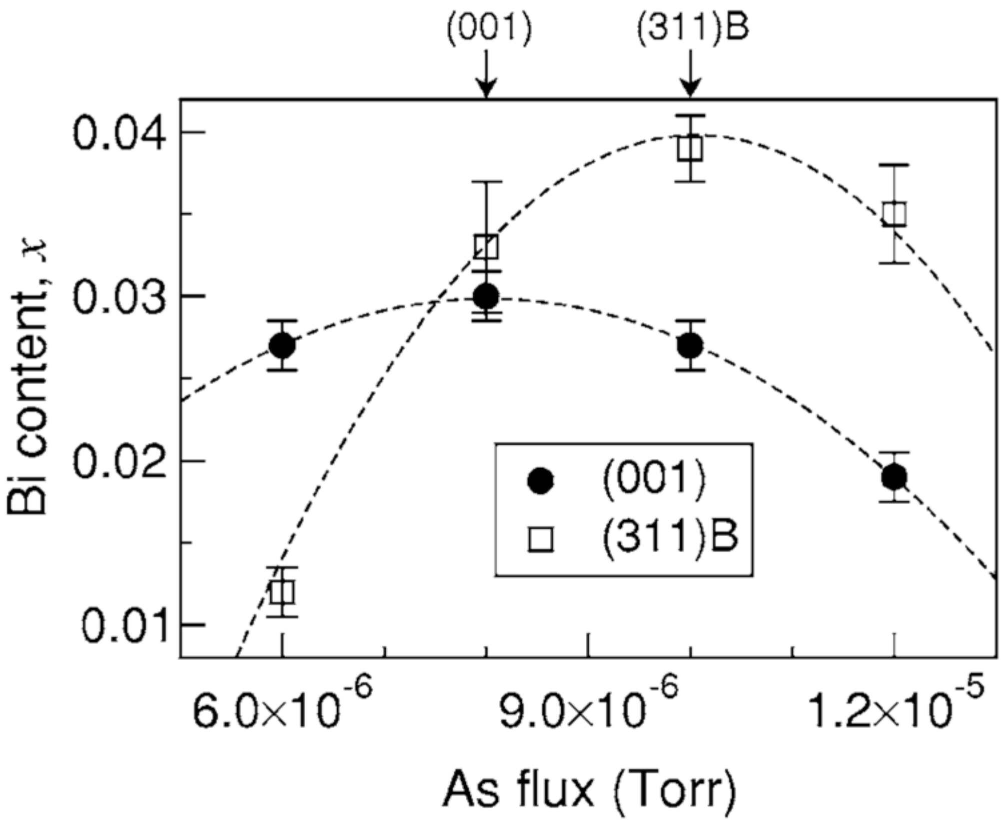

FIG. 2. Bi composition x of different (001) and (311)*B* $GaBi_xAs_{1-x}$ epilayers as a function of the As flux used for the growth. The arrows indicate the As flux for near-stoichiometric growth of (001) and (311)*B* GaAs.

M. Henini *et al.*
Applied Physics Letters
94, 251909 (2007)

GaBiAs

Not transient currents

FIG. 1. Time-domain spectrum of terahertz field radiated from (311)*B* $GaBi_{0.035}As_{0.965}$ sample (transmission geometry). (a) Dependence of peak terahertz field on optical fluence of pump beam (reflection geometry). (b) Dependence of peak terahertz field on angle of in-plane magnetic field (reflection geometry).

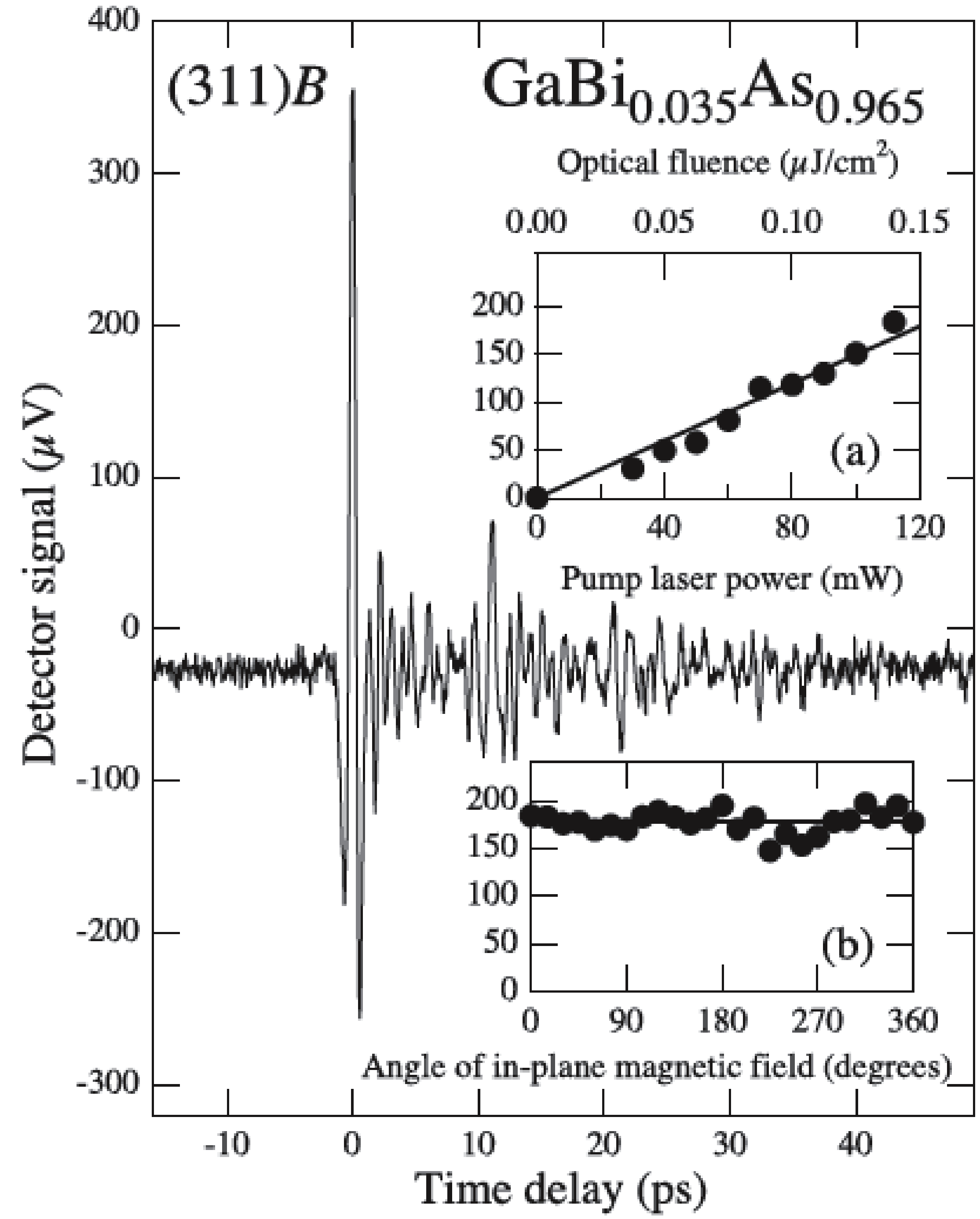

K. Radhanpura, S. Hargreaves, R. A. Lewis, M. Henini
Applied Physics Letters
94, 251115 (2009)

GaBiAs

Azimuthal angle dependence
- epilayer
quite different to substrate

K. Radhanpura, S. Hargreaves, R. A. Lewis, M. Henini
Applied Physics Letters
94, 251115 (2009)

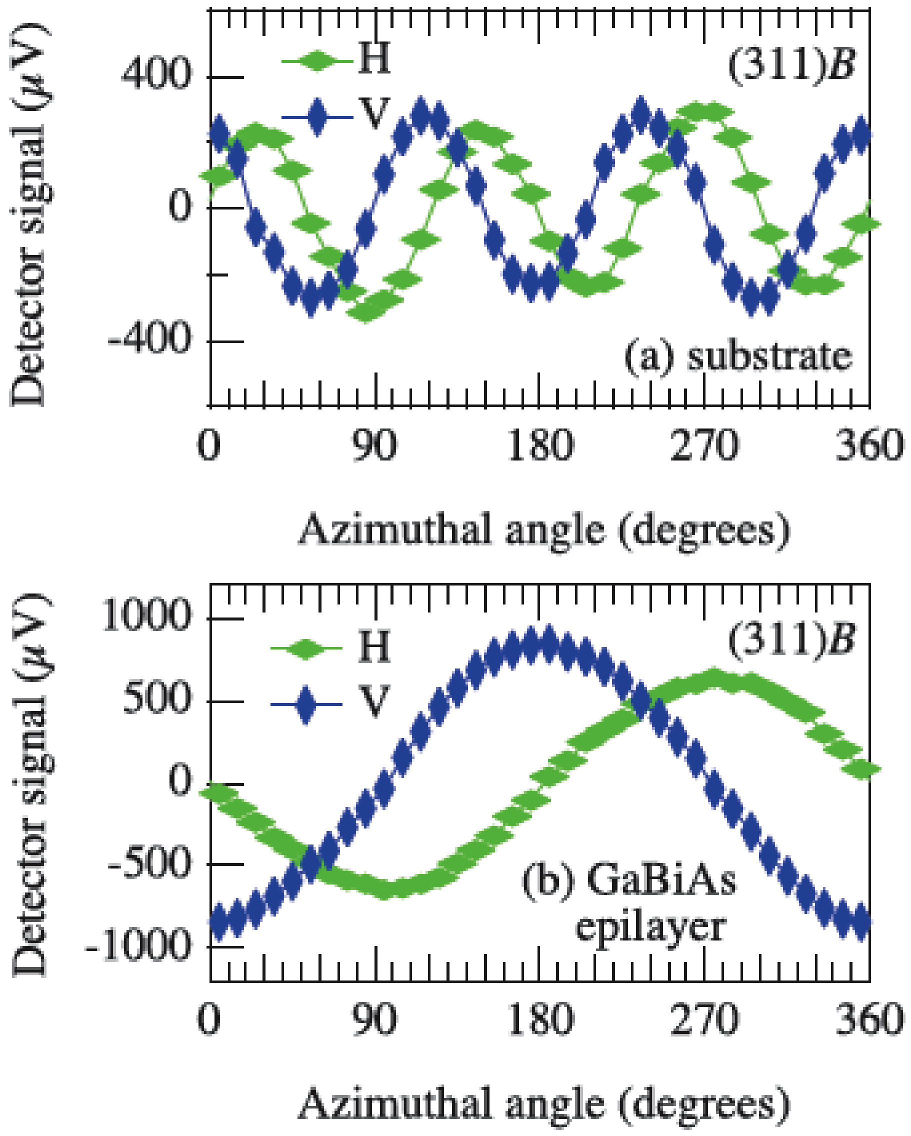

FIG. 2. (Color online) Variation of the peak terahertz field, for both H- and V-polarizations, as a function of angle of rotation around the sample normal in transmission geometry for (311)*B* (a) substrate and (b) $GaBi_{0.035}As_{0.965}$ epilayer.

GaBiAs

$$P_x = 2d_{14}E_yE_z + \alpha' F_x + \beta' E_x + \gamma' E_x^2 F_x, \quad (1)$$

$$P_y = 2d_{14}E_zE_x + \alpha' F_y + \beta' E_y + \gamma' E_y^2 F_y, \quad (2)$$

$$P_z = 2d_{14}E_xE_y + \alpha' F_z + \beta' E_z + \gamma' E_z^2 F_z. \quad (3)$$

(a) Bulk (b) Surface
(c) Sum of bulk and surface

Optical Rectification

K. Radhanpura, S. Hargreaves,
R. A. Lewis, M. Henini
Applied Physics Letters
94, 251115 (2009)

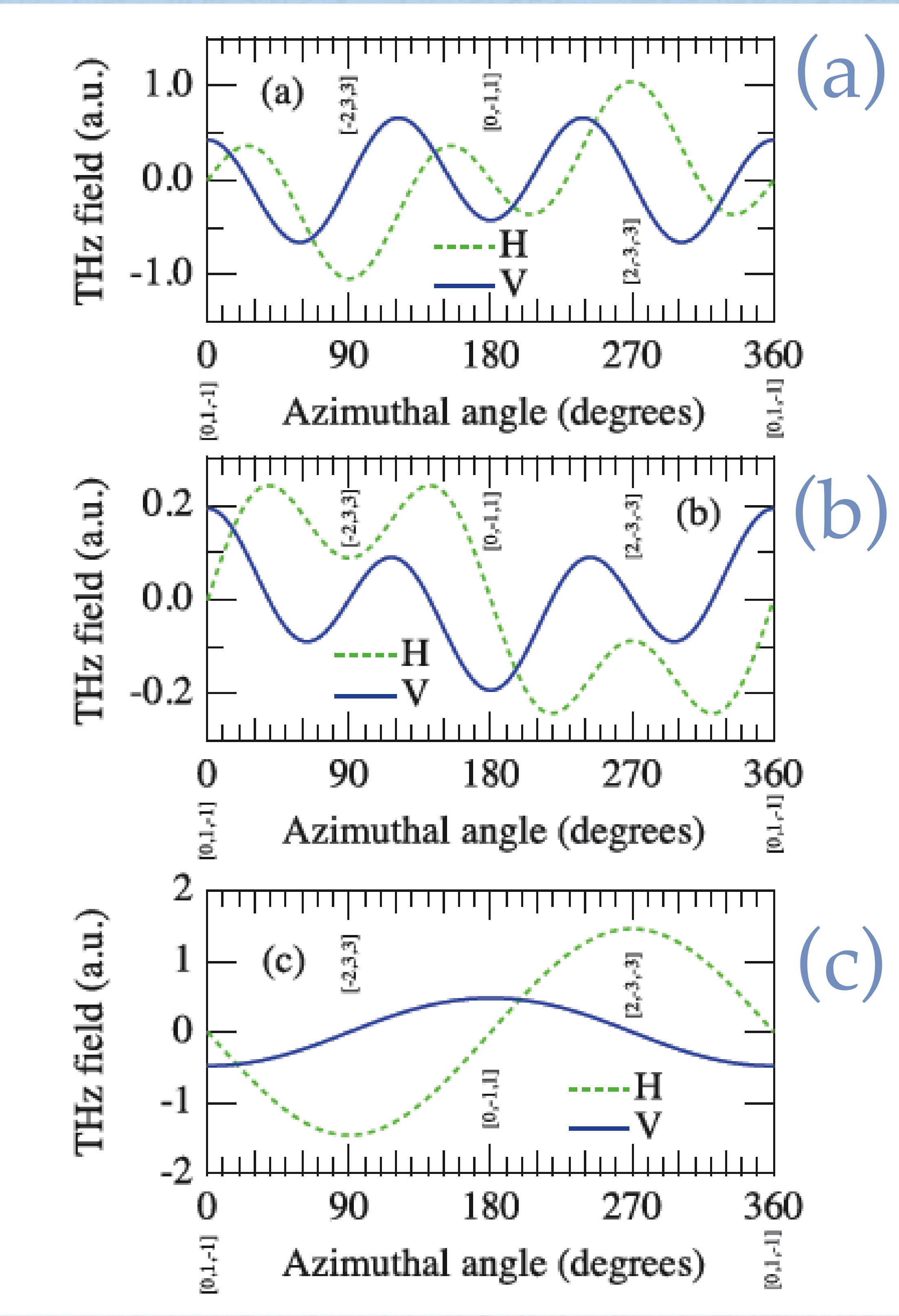

Conclusion

Optical rectification produces THz radiation

THz field emitted is in general polarized and depends in detail on

- angle of incidence of pump beam
- polarization of pump beam
- index *hkl* of crystal face
- azimuthal angle of sample relative to pump beam

In GaBiAs the THz radiated depends strongly on

- crystal face *hkl*
- bulk optical rectification term
- surface field-induced optical rectification term

So THz emission acts as a sensitive surface probe